CROATICA CHEMICA ACTA
CCACAA **76** (1) 93–99 (2003)

ISSN-0011-1643
CCA-2858
Original Scientific Paper

Structural Basis for Selectivity of Butyrylcholinesterase towards Enantiomeric Quinuclidin-3-yl Benzoates: a Quantum Chemical Study

Ines Primožič,* Tomica Hrenar, Srđanka Tomić, and Zlatko Meić

University of Zagreb, Faculty of Science, Department of Chemistry, Strossmayerov trg 14, HR-10000 Zagreb, Croatia

RECEIVED SEPTEMBER 9, 2002; REVISED JANUARY 15, 2003; ACCEPTED JANUARY 17, 2003

Key words
• butyrylcholinesterase
• benzoylcholine
• (*R*)- and (*S*)-quinuclidin-3-yl benzoates
• semiempirical calculations
• Michaelis complexes
• tetrahedral intermediates
• mechanism of hydrolysis

In order to explain different rates of hydrolysis of (*R*)- and (*S*)-quinuclidin-3-yl benzoates and benzoylcholine catalyzed with butyrylcholinesterase, semiempirical PM3 calculations were performed with an assumed active site model of human BChE (20 amino acids). Contributions of different protein residues to the stabilization of Michaelis complexes and tetrahedral intermediates were analyzed. It was shown that the hydrolysis rates of quinuclidinium enantiomers were to an appreciable extent affected by the existence or absence of the hydrogen bond between the quinuclidinium N^+–H group and the protein residues. Calculations indicated that the better stabilization of quinuclidinium moiety in the Michaelis complex than in the tetrahedral intermediate was the main reason for a greater barrier and a slower reaction rate of the (*R*)-enantiomer of quinuclidinium esters compared to benzoylcholine. In the case of (*S*)-enantiomer, the calculation indicated that the barrier to the substrate reorientation from a favourable, but non-productive binding to a productive one significantly influenced the rate of hydrolysis.

INTRODUCTION

Butyrylcholinesterase (BChE, EC 3.1.1.8) is a serine hydrolase closely related with acetylcholinesterase (AChE, EC 3.1.1.7).[1] Although the physiological function of BChE is not clear, it most likely serves to hydrolize some toxic dietary esters.[2] AChE and BChE share about 55 % of amino acids sequence identity in mammalian species. Therefore, based on the resolved crystal structure of various AChE, a three dimensional homology model of BChE can be built.[3]

It has been shown for BChE that it can accept compounds of diverse structures as substrates. In the case of esters, BChE hydrolyzes positively charged choline esters (from acetyl to heptanoyl and benzoyl esters), some neutral esters (*e.g.*, α-naphtyl acetate and *o*-nitrophenyl butyrate) and degrades several ester drugs of interest, such as cocaine, heroin, aspirin, procaine and succinylcholine.[4] Furthermore, BChE has been investigated as a catalyst in organic synthesis.[5–7] Among the substrates tested were the esters of quiniclidin-3-ol, which embody the functional groups of acetylcholine in a semirigide structure. It was shown that BChE preferentially hydrolyzes (*R*)-enantiomers of chiral quinuclidinol esters. In the case of chiral quinuclidin-3-yl benzoates and benzoylcholine, specificity constants (k_{cat}/K_M) revealed that the acylation step proceeds 7-fold slower for (*R*)- and a 55-fold slower for (*S*)-enantiomer of quinuclidin-3-yl benzoates compared to benzoylcholine.[7]

The present study was designed to evaluate the molecular basis for selectivity of BChE-catalyzed hydrolysis of chiral quinuclidin-3-yl benzoates (RQBz and SQBz)

* Author to whom correspondence should be addressed. (E-mail: ines@chem.pmf.hr)

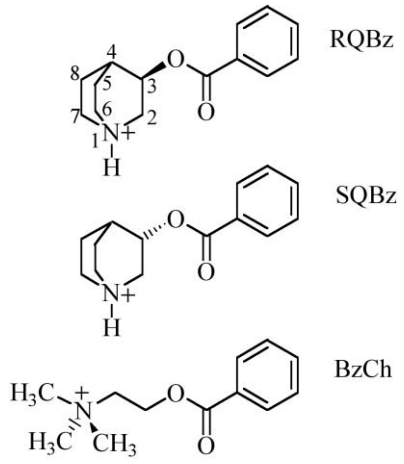

Figure 1. Ligands chosen for the semiempirical calculations.

and benzoylcholine (BzCh), Figure 1. Although the performed docking simulations did reveal some of the important interactions of benzoates with the enzyme, it was not possible to explain the differences in the reaction rates of the tested esters.[7] Therefore, we decided to build a model of the active site of BChE and to optimize the structures of Michaelis complexes (MC) and tetrahedral intermediates (TI) for all compounds at the semiempirical level. It was assumed that the interactions in the ground states would reflect the differences in the rates of acylation between enantiomers and BzCh. The chosen model and the used method of calculation were selected to gain a good compromise between accuracy and the time necessary for the calculation.

EXPERIMENTAL

Geometry optimizations of Michaelis complexes (MC) and tetrahedral intermediates (TI) of all compounds were carried out using semiempirical calculations (PM3)[8] with the Gaussian98 quantum chemical program.[9] The molecular mechanics correction for the peptide linkages was included. All calculations were performed on the PC Dual AMD 1900+ MP.

Amino acids used to create the active site of the enzyme were taken from the reported three-dimensional homology-built model of human BChE.[3] Thus, BChE residues bear the Torpedo californica AChE numbering. Actual numbers of human BChE residues are given in parentheses. The following amino acids were used and modified: Asp72 (70), Ser81 (79), Trp84 (82), Gly118 (116), Gly119 (117), Tyr130 (128), Glu199 (197), Ser200 (198), Ala201 (199), Trp233 (231), Leu288 (286), Glu327 (325), Ala330 (328), Phe331 (329), Tyr334 (332), Phe400 (398), Trp432 (430), Met439 (437), His440 (438) and Gly441 (439). The modification procedure included: (i) addition of formyl or amino group to every free α-amino and α-carboxyl group to model the peptide backbone, (ii) aromatic amino acids (except His440) were represented only by the appropriate aromatic ring and the β-carbon atom as methyl group, and (iii) in TI, covalent bond between γ-oxygen atom of Ser200 and the ligand was created and the hydrogen atom from the serine hydroxyl group was transferred to the nitrogen atom of His440. To ensure that the positions of amino acids would remain as those in the enzyme, some atom positions were frozen during the optimization: (i) terminal carbon and nitrogen atoms of all amino acids, (ii) C1 atom of the phenyl ring and nitrogen atom of the indole ring, (iii) nitrogen atoms of Gly118, Gly119 and Ala201, (iv) β-carbon atom of Ser200, and (v) δ-carbon atom of Glu199.

RESULTS AND DISCUSSION

In this study, hydrolyses of esters by BChE were described by the simplified kinetic model where the three-step mechanism was considered, Scheme 1.[10] E, MC, and EA represent the free enzyme, Michaelis complex and acylenzyme intermediate, respectively, S is the substrate and P^1 and P^2 are the respective alcohol and acid products of the hydrolysis.

$$E + S \underset{k_{-1}}{\overset{k_1}{\rightleftharpoons}} MC \xrightarrow{k_2} EA + P^1 \xrightarrow[H_2O]{k_3} E + P^2$$

Scheme 1.

The results of our kinetic study showed that the difference in k_{cat} of the benzoate esters tested, Figure 1, lays in a slower benzoylation of BChE since the debenzoylation of the enzyme was the same for all substrates.[7] Therefore, we decided to investigate the initial stages of catalysis, Michaelis complexes (MC) and tetrahedral intermediates (TI) as proposed in Scheme 2.[10] It is believed that enzymes interact more strongly with transition

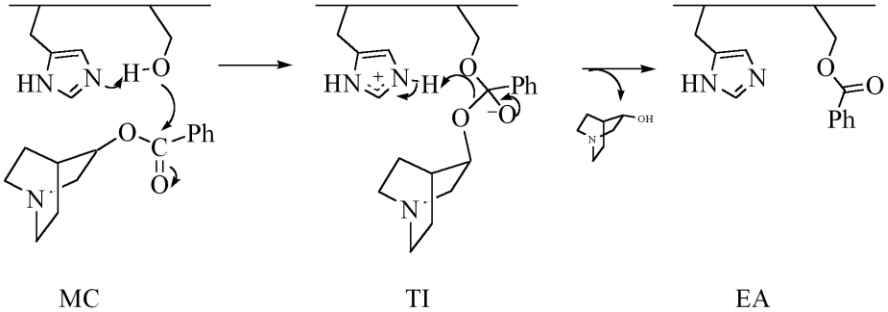

Scheme 2.

states than with ground states and when a mechanism involves formation of an unstable intermediate, the transition state closely resembles that intermediate.[11] Thus, we assumed that the stability of TI would reflect the observed differences in hydrolysis rates and specificity constants of enantiomers.

The model of the BChE active site was limited to 20 amino acids whose Cartesian coordinates were taken from the homology-built 3D model of human BChE.[3] These amino acids make specific contributions to the substrate specificity and catalytic power of the enzyme.[1] They form four major domains of the BChE active site: (i) the esteratic site containing active serine as part of the catalytic triad (Ser200, His440, Glu327), (ii) the acyl pocket (Leu285, Trp233, Phe400, Phe331) – a hydrophobic region which accommodates the acyl group of an ester, (iii) the choline subsite (Trp84, Tyr130, Glu199), the recognition of the substrate's quaternary ammonium group, and (iv) the oxyanion hole formed by the main chain N–H dipoles (Gly118, Gly119, Ala201) interacting with the negatively charged carbonyl oxygen of the substrate in a tetrahedral intermediate.[1]

Computational studies on enyzme reactions were successfully done using the semiempirical AM1[12] method as well as the PM3[13] method. Therefore, in order to determine the better choice between the AM1 and PM3 methods, test calculations were done. We have calculated the MC complex and the TI intermediate of BzCh with both methods. Comparison of the geometries obtained showed that the more accurate description of the active site interactions was obtained with the PM3 method. The results confirmed that the greatest difference was the inferior description of hydrogen bonds as calculated with the AM1 method.[13a,14] For instance, AM1 calculations predicted 3.40 and 2.95 Å in MC, and 3.14 and 2.90 Å in TI for the catalytic triad O_γ(Ser200)–$N_{\varepsilon 2}$(His440) and $N_{\delta 1}$(His440)–$O_{\varepsilon 1}$(Glu327) distances, respectively. On the other hand, much stronger hydrogen bonds were obtained by PM3 calculations, Table I, whose values were in excellent agreement with the X-ray data for AChE complexes[15] and catalytic triads of related enzymes such as trypsine and α-chymotripsin.[16] Therefore, since we modeled the catalytic triad (two hydrogen bonds) and oxyanion hole interactions (three hydrogen bonds expected in tetrahedral intermediates), we decided to use semiempirical PM3 calculations to estimate the ligand orientation and the relative energies for Michaelis complexes and tetrahedral intermediates. Only similar orientations with respect to the benzoyl part of the ligand, which are assumed to lead to the formation of tetrahedral intermediates, were calculated (MC). One additional possible binding (MC-2) of the worst substrate (SQBz) was proposed in order to find an explanation for its slowest hydrolysis kinetics. The obtained relative energies for MC and TI for all ligands are displayed in Figure 2.

Analyses of the obtained complexes revealed numerous close contacts of ligands with the enzyme residues in the active site model.

Acyl Binding Pocket

Since all calculated ligands were esters of benzoic acid, the similar position and interactions of phenyl ring and carbonyl group were expected. Phenyl group of all ligands in MC complexes and TI intermediates fitted very tightly into the acyl binding pocket. In both non-covalent and covalent adducts, the phenyl ring was directed towards and made a T-shaped aromatic complex with the Trp233 and close contacts with all other amino acids in the acyl pocket including the Gly119.

Catalytic Triad

Although the initial distances between O_γ (Ser200) and $N_{\delta 2}$ (His440) were 3.50 Å and $N_{\varepsilon 1}$ (His440) and $O_{\varepsilon 1}$ (Glu327) 3.25 Å, in the optimized structures of MC complexes they were ≈2.80 and ≈2.70 Å, respectively, Table I. Upon ligand binding and protonation of His440, an even stronger hydrogen bond between His440 and Glu327 was formed, as expected. This assured us that there was enough flexibility in our model and confirmed that our calculations produced results consistent with the known features of the catalytic triads of serine hydrolases.[15]

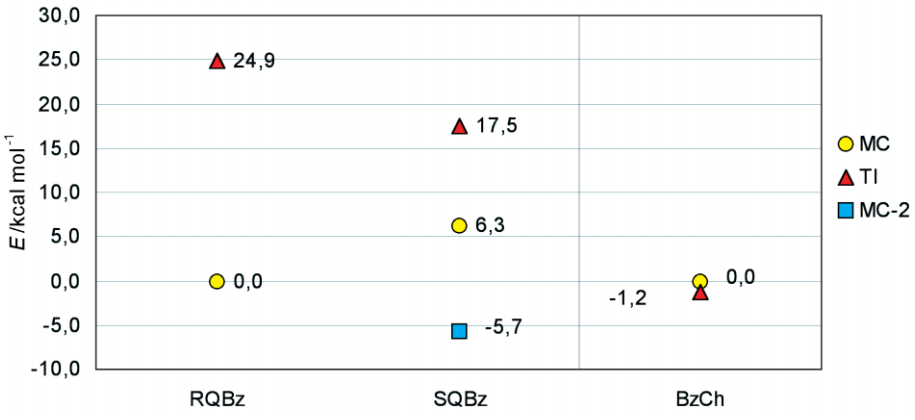

Figure 2. PM3 calculated values of relative energies of the Michaelis complexes (MC, MC-2) and tetrahedral intermediates (TI) obtained for RQBz, SQBz and BzCh. RQBz MC complex was used as a reference point for both quinuclidinium ligands. The energy of BzCh TI intermediate is relative to that of BzCh MC complex.

TABLE I. Esteratic site. Selected interatomic distances (*d*/Å) for Michaelis complexes (MC) and tetrahedral intermediates (TI) for all ligands (L; RQBz, SQBz, BzCh)[a], calculated by the PM3 method

	RQBz		SQBz			BzCh	
	MC	TI	MC	MC-2	TI	MC	TI
O_{γ}–H(Ser200)	0.98	1.78	0.97	0.97	1.82	0.97	1.76
$N_{\varepsilon 2}$(His440)–H_{γ}(Ser200)	1.78	1.02	1.80	1.81	1.02	1.79	1.01
$N_{\delta 1}$–$H_{\delta 1}$(His440)	1.03	1.04	1.03	1.03	1.05	1.03	1.04
$O_{\varepsilon 1}$(Glu327)–$N_{\delta 1}$(His440)	2.70	2.66	2.70	2.70	2.66	2.71	2.66
$C_{carbonyl}$(L)–O_{γ}(Ser200)	3.39	1.45	3.18	5.31	1.46	3.24	1.44

(a) RQBz and SQBz, quinuclidine benzoates; BzCh, benzylcholine (see Figure 1).

TABLE II. Oxyanion hole. Selected interatomic distances (*d*/Å) for Michaelis complexes (MC) and tetrahedral intermediates (TI) for all ligands (L; RQBz, SQBz, BzCh)[a], calculated by the PM3 method

	RQBz		SQBz			BzCh	
	MC	TI	MC	MC-2	TI	MC	TI
$O_{carbonyl}$(L)–N(Ala201)	4.58	2.83	4.18	6.47	2.84	4.51	2.82
N–H(Ala201)	1.00	1.03	1.00	1.00	1.03	1.00	1.03
$O_{carbonyl}$(L)–N(Gly118)	2.89	2.75	2.73	3.42	2.77	2.78	2.76
N–H(Gly118)	1.00	1.03	1.00	1.00	1.02	1.01	1.02
$O_{carbonyl}$(L)–N(Gly119)	2.88	2.73	2.75	2.76	2.79	2.77	2.76
N–H(Gly119)	1.02	1.03	1.01	1.01	1.03	1.01	1.03

(a) RQBz and SQBz, quinuclidine benzoates; BzCh, benzylcholine (see Figure 1).

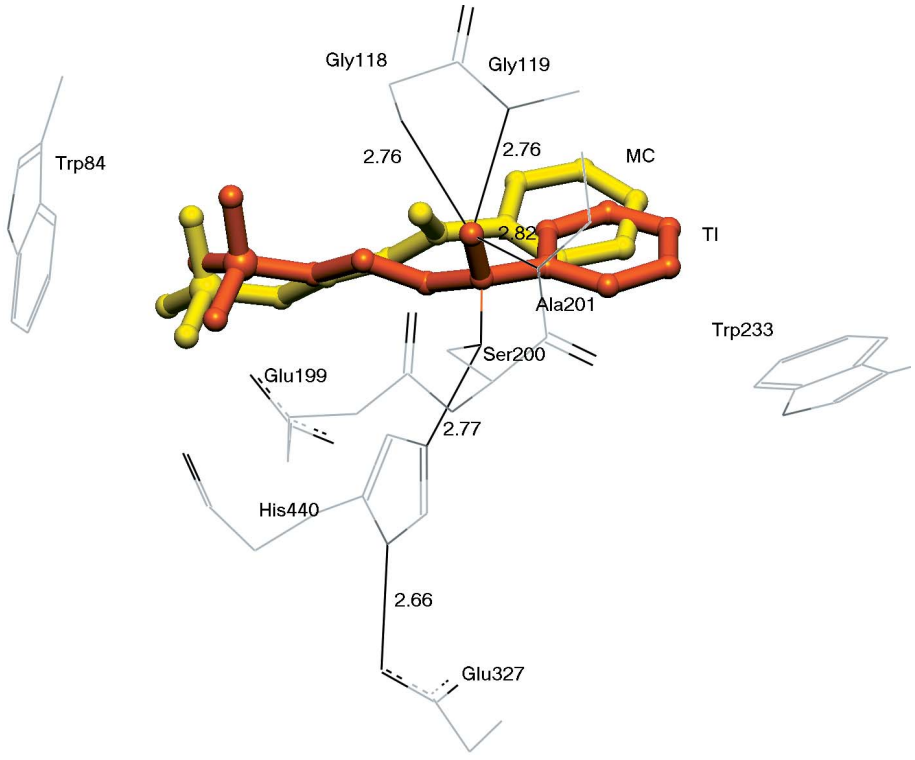

Figure 3. Orientations of the BzCh Michaelis complex (MC, yellow) and tetrahedral intermediate (TI, orange) in the model of the BChE active site represented by some structurally important amino acids obtained by PM3 calculations for TI intermediate. The ball and stick model represents the ligand with a nitrogen atom highlighted. Hydrogen atoms are omitted for clarity. Interatomic distances are given in Å.

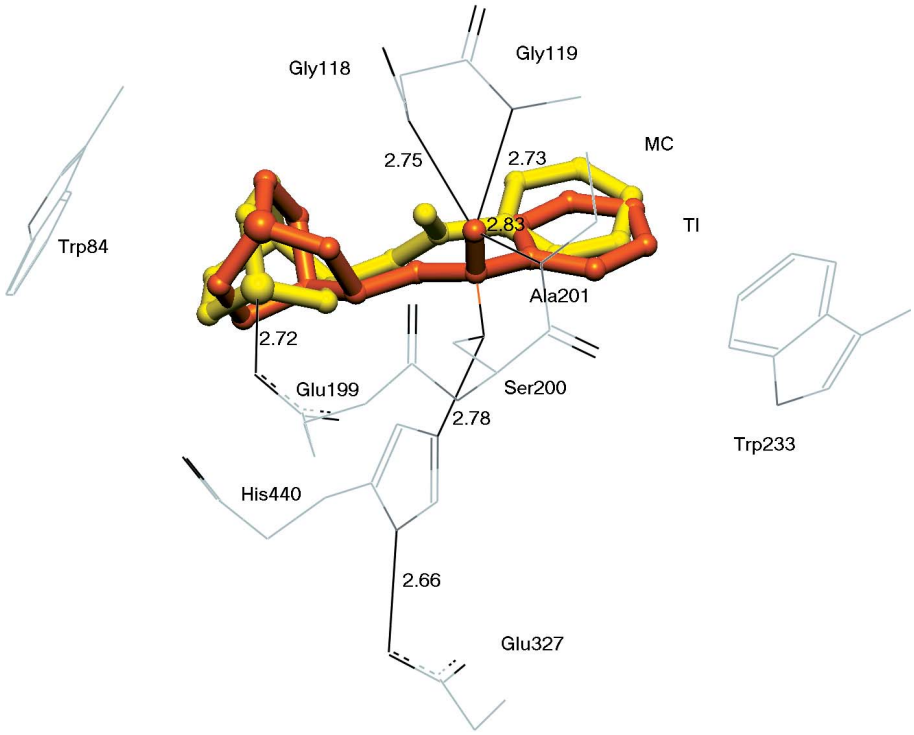

Figure 4. Orientations of the RQBz Michaelis complex (MC, yellow) and tetrahedral intermediate (TI, orange) in the model of the BChE active site represented by some structurally important amino acids obtained by PM3 calculations for TI intermediate. The ball and stick model represents the ligand with a nitrogen atom highlighted. Hydrogen atoms are omitted for clarity. Interatomic distances between atoms of ligand and amino acids are given in Å.

Oxyanion Hole

Besides the hydrogen bonds in the catalytic triad, our model predicted the hydrogen bonds in the oxyanion hole,[1] as well. TI intermediates are characterized by three hydrogen bonds between the negatively charged carbonyl oxygen atom of the ligand and three components of the oxyanion hole (Gly118, Gly119 and Ala201), Table II, Figures 3, 4 and 5. In MC complexes, the carboxyl oxygen atom is also situated toward the oxyanion hole in a position suitable for nucleophilic attack by the active serine. There are weak hydrogen bonds between the carboxyl oxygen of a ligand and the amide backbone of Gly118 and Gly119, Table II.

Choline Binding Subsite

It is clear that the obtained PM3 interaction energies of two enantiomers are functions of intermolecular distances in the choline binding site, Table III. Comparison of interatomic distances between the ligands and the selected residues in the choline subsite revealed that smaller quinuclidinium moiety interacts more weakly with the Trp84 than with the BzCh quaternary ammonium group. However, interaction with the Glu199 was very strong for quinuclidinium compounds compared to choline ester. In the MC complex of RQBz, quinuclidinium part is oriented in such a way that a strong hydrogen bond between quinuclidinium nitrogen and Glu199 carboxyl group is

TABLE III. Choline subsite. Selected interatomic distances (*d*/Å) for Michaelis complexes (MC) and tetrahedral intermediates (TI) for all ligands (L; RQBz, SQBz, BzCh), calculated by the PM3 method

	RQBz[a]		SQBz[a]			BzCh[b]	
	MC	TI	MC	MC-2	TI	MC	TI
N^+(L)–O(Glu199)	2.72	3.50	3.60	2.66	3.47	4.70	3.97
C_2(L)–O(Glu199)	2.83	3.28	2.91	3.71	2.87	3.50	2.76
C_6(L)–O(Glu199)	3.83	4.94	5.06	3.57	4.94	5.17	4.39
C_7(L)–O(Glu199)	3.44	2.86	2.91	3.09	2.89	5.93	5.20
N^+(L)–indole centre(Trp84)	4.85	4.80	4.58	5.62	4.67	4.22	4.23
C_2(L)–indole centre(Trp84)	6.14	6.26	6.03	6.59	6.16	4.11	4.15
C_6(L)–indole centre(Trp84)	4.47	4.65	4.13	5.42	4.45	3.60	4.16
C_7(L)–indole centre(Trp84)	3.94	4.10	4.09	4.45	4.20	4.24	3.62

[a] See Figure 1 for notation of the quinuclidinium ring atoms. [b] C_2, C_6 and C_7 for BzCh represent distances from the quaternary ammonium methyl carbon atoms of the ligand to the centre of the indole ring (Trp84).

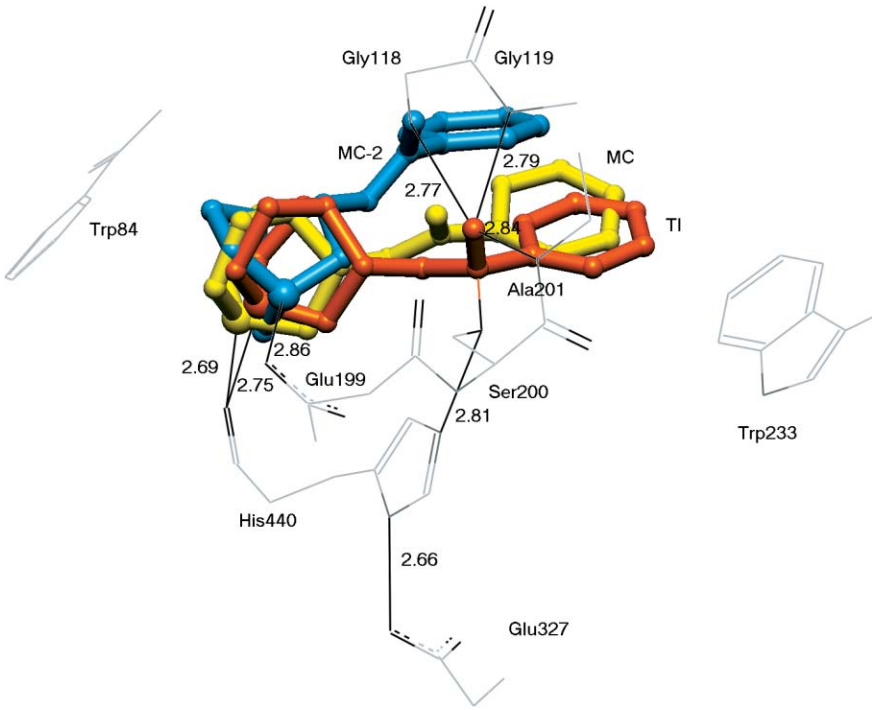

Figure 5. Orientations of the SQBz Michaelis complexes (MC, yellow and MC-2 blue) and tetrahedral intermediate (TI, orange) in the model of the BChE active site represented by some structurally important amino acids obtained by PM3 calculations for TI intermediate. The ball and stick model represents the ligand with a nitrogen atom highlighted. Hydrogen atoms are omitted for clarity. Interatomic distances between atoms of ligand and amino acids are given in Å.

formed, the distance being 2.72 Å, Figure 4. Steric requirements of the choline subsite prevent formation of that hydrogen bond in SQBz MC complex, which is necessary for the reaction to occur *via* a stabilized transition state in the oxyanion hole, Figure 5. Instead, a weaker complex with a hydrogen bond between quinuclidinium N–H group and carboxyl oxygen atom of His440 was formed (2.69 Å, N^+–H bond lenght 1.02 Å). When we reoriented the ligand and allowed the hydrogen bond with the Glu199 to be formed, the resulting MC-2 complex had a significantly lower energy, but this caused elongation of the distance from the carboxyl group of the ligand to the hydroxyl group of catalytic Ser200 to 5.31 Å, Table I, Figure 5.

In the TI intermediates, there is a closer proximity of SQBz quinuclidinium quaternary ammonium group to Trp84 and Glu199 than that of RQBz, Table III. In addition, in the TI intermediate of SQBz, the hydrogen bond between the quinuclidinium N^+–H group and His440 carboxyl group (2.75 Å, N^+–H bond lenght 1.02 Å) remained, while there was no stabilization of quinuclidinium N^+–H group with a hydrogen bond in the TI intermediate of RQBz, Figures 4 and 5.

Although the TI intermediate of SQBz, according to our model, appeared to be more stabilized than that of RQBz, Figure 2, unfavourable interactions in the MC complex and the possibility of much stronger interactions with the choline subsite (MC-2) indicated that the rate of hydrolysis would be greatly influenced by reorientation of the SQBz MC complex. In the case of BzCh, the quaternary ammonium group is stabilized by a close contact with Trp84 equally in the MC complex and TI intermediate (average distance ≈4.0 Å) while TI intermediate is additionally stabilized by a closer contact with Glu199 (average distance ≈4.8 Å and 4.1 Å in MC and TI, respectively, Table III, Figure 3). On the other hand, the hydrogen bond between quinuclidinium nitrogen and Glu199 carboxylate, which stabilizes the MC complex of RQBz, might be one of the reasons for a slower hydrolysis of RQBz compared to BzCh. This ground state stabilization (MC), which is not followed by the transition state stabilization, caused a greater barrier and a slower reaction rate, Figure 4.

CONCLUSION

In this study, similarities, differences and relations among the obtained orientations of quinuclidin-3-ol and choline benzoates within the active site regions of BChE model were discussed. Quaternary nitrogen atoms of quinuclidine moieties showed a strong tendency to form a hydrogen bond with protein residues. Structures in which a hydrogen bond between quinuclidinium N^+–H group and Glu199 existed proved to be the most stable. Such stabilization of the RQBz MC complex, which did not exist in TI, was expected to be responsible for the decrease of the reaction rate in comparison to BzCh. In the case of (*S*)-enantiomer, the strongest interaction with the choline subsite was not present in the orientation of the complex necessary for the reaction to occur *via* TI. Therefore, it can be assumed that the acylation step is additionally rate limited by the free energy spent on the pre-organization of that ligand. These aspects obviously play an important role in the selectivity of BChE toward enantiomeric quinuclidin-3-yl benzoates.

Acknowledgments. – We thank Professor Israel Silman of the Weizmann Institute, Rehovot, Israel for providing coordinates of the theoretical structure of human BChE. This work was supported by the Ministry of Science and Technology of the Republic of Croatia, Project Nos 119610 and 119641.

REFERENCES

1. P. Taylor and Z. Radić, *Annu. Rev. Pharmacol. Toxicol.* **34** (1994) 281–320.
2. M. Schwarz, D. Glick, Y. Lowenstein and H. Soreq, *Pharmacol. Ther.* **67** (1995) 283–322.
3. M. Harel, J. L. Sussman, E. Krejci, S. Bon, P. Chanal, J. Massoulie, and I. Silman, *Proc. Natl. Acad. Sci. USA* **89** (1992) 10827–10831.
4. O. Lockridge, *Pharmacol. Ther.* **47** (1990) 35–60.
5. M. Schelhaas, S. Glomsda, M. Hänsler, H.-D. Jakubke, and H. Waldmann, *Angew. Chem., Int. Ed. Engl.* **35** (1996) 106–109.
6. M. Rehavi, S. Maayani, and M. Sokolovsky, *Life Sci.* **21** (1977) 1293–1302.
7. I. Primožič, T. Hrenar, S. Tomić, and Z. Meić, *J. Phys. Org. Chem.* **58** (2002) 608–614.
8. J. J. P. Stewart, *J. Comput. Chem.* **10** (1998) 209–221.
9. M. J. Frisch, G. W. Trucks, H. B. Schlegel, G. E. Scuseria, M. A. Robb, J. R. Cheeseman, V. G. Zakrzewski, J. A. Montgomery, Jr., R. E. Stratmann, J. C. Burant, S. Dapprich, J. M. Millam, A. D. Daniels, K. N. Kudin, M. C. Strain, O. Farkas, J. Tomasi, V. Barone, M. Cossi, R. Cammi, B. Mennucci, C. Pomelli, C. Adamo, S. Clifford, J. Ochterski, G. A. Petersson, P. Y. Ayala, Q. Cui, K. Morokuma, D. K. Malick, A. D. Rabuck, K. Raghavachari, J. B. Foresman, J. Cioslowski, J. V. Ortiz, A. G. Baboul, B. B. Stefanov, G. Liu, A. Liashenko, P. Piskorz, I. Komaromi, R. Gomperts, R. L. Martin, D. J. Fox, T. Keith, M. A. Al-Laham, C. Y. Peng, A. Nanayakkara, C. Gonzalez, M. Challacombe, P. M. W. Gill, B. Johnson, W. Chen, M. W. Wong, J. L. Andres, C. Gonzalez, M. Head-Gordon, E. S. Replogle, and J. A. Pople, Gaussian 98, Revision A.7, Gaussian, Inc., Pittsburgh PA, 1998.
10. D. M. Quinn, *Chem. Rev.* **87** (1987) 955–979.
11. A. Warshel, *J. Biol. Chem.* **273** (1998) 27035–27038.
12. (a) L. Ridder, A. J. Mulholland, J. Vervoort, and I. M. C. M. Rietjens, *J. Am. Chem. Soc.* **120** (1998) 7641–7642. (b) S. Antonczak, G. Monard, M. F. Ruiz-Lopez, and J.-L. Rivail, *J. Am. Chem. Soc.* **120** (1998) 8825–8833.
13. (a) J. Andres, V. Moliner, J. Krechl, and E. Silla, *J. Chem. Soc., Perkin Trans. 2* (1995) 1551–1558. (b) K. M. Jr. Merz and L. Banci, *J. Phys. Chem.* **100** (1996) 17414–17420.
14. M. Garcia-Viloca, A. Gonzales-Lafont, and J. M. Lluch, *J. Am. Chem. Soc.* **123** (2001) 709–721.
15. (a) M. Harel, D. M. Quinn, H. K. Nair, I. Silman, and J. L. Sussman, *J. Am. Chem. Soc.* **118** (1996) 2340–2346. (b) M. L. Raves, M. Harel, Y. P. Pang, I. Silman, A. P. Kozikowski, and J. L. Sussman, *Nat. Struct. Biol.* **4** (1997) 57–63.
16. H. Tusukada and D. M. Blow, *J. Mol. Biol.* **184** (1985) 703–711.

SAŽETAK

Strukturni temelj selektivnosti butirilkolinesteraze prema enantiomernim kinuklidin-3-il-benzoatima: kvantno-kemijsko istraživanje

Ines Primožič, Tomica Hrenar, Srđanka Tomić i Zlatko Meić

Da bi objasnili različite brzine hidroliza (*R*)- i (*S*)-kinuklidin-3-il-benzoata i benzoilkolina kataliziranih butirilkolinesterazom, optimirane su geometrije i izračunane energije Michaelisovih kompleksa i tetraedrijskih međuprodukata za koje se pretpostavlja da nastaju tijekom hidrolize. Metoda upotrebljena za optimizaciju bila je semiempirijska PM3 metoda. Model aktivnoga mjesta sastojao se od 20 odabranih aminokiselina unutar aktivnoga mjesta butirilkolinesteraze. Pokazalo se da je hidroliza enantiomernih estera kinuklidina u značajnoj mjeri određena postojanjem ili odsustvom vodikove veze između kinuklidinijeve amino skupine i okolnih aminokiselina. Nađeno je da se razlika u brzini hidrolize između (*R*)-enantiomera i benzoilkolina može objasniti dodatnom stabilizacijom Michaelisovoga kompleksa (*R*)-estera kinuklidina koja izostaje u njegovom tetraedrijskom međuproduktu. To ima za posljedicu višu barijeru za reakciju i sporiju hidrolizu. Jače stabilizirani Michaelisov kompleks (*S*)-enantiomera nije pogodan za reakciju pa je brzina hidrolize ovog estera određena u velikoj mjeri i brzinom reorijentacije unutar aktivnoga mjesta.